Uncialamycin-based antibody–drug conjugates: Unique enediyne ADCs exhibiting bystander killing effect

K. C. Nicolaou[a,1], Stephan Rigol[a], Emmanuel N. Pitsinos[a,b], Dipendu Das[a], Yong Lu[a], Subhrajit Rout[a], Alexander W. Schammel[c,2], Dane Holte[c], Baiwei Lin[d,2], Christine Gu[d], Hetal Sarvaiya[d], Jose Trinidad[d,2], Nicole Barbour[d,2], Amanda M. Valdiosera[d,2], Joseph Sandoval[e,2], Christina Lee[e], Monette Aujay[e,2], Hanan Fernando[f,2], Anukriti Dhar[f,2], Holger Karsunky[f,2], Nicole Taylor[g,2], Marybeth Pysz[g], and Julia Gavrilyuk[c,1]

[a]BioScience Research Collaborative, Department of Chemistry, Rice University, Houston, TX 77005; [b]Laboratory of Natural Products Synthesis & Bioorganic Chemistry, Institute of Nanoscience and Nanotechnology, National Centre for Scientific Research "Demokritos", 153 10 Agia Paraskevi, Greece; [c]Discovery Chemistry Department, AbbVie Inc., South San Francisco, CA 94080; [d]Bioconjugation and Process Development Department, AbbVie Inc., South San Francisco, CA 94080; [e]Assay Development Department, AbbVie Inc., South San Francisco, CA 94080; [f]Cancer Biology Department, AbbVie Inc., South San Francisco, CA 94080; and [g]In Vivo Pharmacology Department, AbbVie Inc., South San Francisco, CA 94080

Contributed by K. C. Nicolaou, May 11, 2021 (sent for review April 15, 2021; reviewed by E. J. Corey, Sanjeev Gangwar, Scott J. Miller, and Ian Paterson)

Antibody–drug conjugates (ADCs) have emerged as valuable targeted anticancer therapeutics with at least 11 approved therapies and over 80 advancing through clinical trials. Enediyne DNA-damaging payloads represented by the flagship of this family of antitumor agents, *N*-acetyl calicheamicin γ_1^I, have a proven success track record. However, they pose a significant synthetic challenge in the development and optimization of linker drugs. We have recently reported a streamlined total synthesis of uncialamycin, another representative of the enediyne class of compounds, with compelling synthetic accessibility. Here we report the synthesis and evaluation of uncialamycin ADCs featuring a variety of cleavable and noncleavable linkers. We have discovered that uncialamycin ADCs display a strong bystander killing effect and are highly selective and cytotoxic in vitro and in vivo.

antibody–drug conjugates | bystander killing effect | enediyne payloads

Although the essential concept of antibody–drug conjugates (ADCs) was proposed by Paul Ehrlich more than a century ago (1), it was only at the dawn of the 21st century that this concept was translated into a targeted cancer therapy when Mylotarg (2, 3) was approved for clinical use for the treatment of acute myeloid leukemia. Since then a number of other ADCs have been approved as clinical therapies (4), including Adcetris (5), Kadcyla (6), Besponsa (7), Polivy (8), Padcev (9), Enhertu (10), Trodelvy (11), Blenrep (12), Lumoxiti (13), and Zynlonta (14). These successes emerged as a result of multidisciplinary efforts to ensure fine-tuning and optimizing the various components of the ADCs, including the payload, the linker, the linker-drug, the antibody, and the final ADC. The approval of Mylotarg (carrying the N-acetylated version of calicheamicin γ_1^I [**1**], *N*-acetyl calicheamicin γ_1^I [**2**], as the payload) by the Food and Drug Administration in 2000 validated our earlier disclosure of an ADC (15) carrying a totally synthetic thioacetate analog (calicheamicin θ_1^I [**3**]) (16) of calicheamicin γ_1^I (**1**) that exhibited suppression of growth and dissemination of liver metastases in a syngeneic model of murine neuroblastoma. Inspired by these calicheamicin γ_1^I payloads, and their ADCs, we undertook the total synthesis (17, 18) of uncialamycin (19) (**4**; Fig. 1), a natural product whose structure resembles that of calicheamicin γ_1^I with regard to the 10-membered ring enediyne structural motif. Our asymmetric and successful total synthesis of uncialamycin (18) facilitated not only its absolute configuration assignment but also the design, synthesis, and biological evaluation of numerous uncialamycin analogs. From these diverse structures, methylamine analog **5** (Fig. 1) was chosen as a payload for further advancement and investigation by virtue of its high potency and convenient handle for linker attachment. The envisioned sequence was to include linker-drug design and synthesis, attachment onto appropriate antibodies to afford ADCs, and in vitro and in vivo biological evaluation as targeted anticancer agents.

Results and Discussion

Design and Synthesis of Linker-Drugs LD1 to LD6. Applying our developed synthetic strategies and technologies for the synthesis of uncialamycin, and following the reported protocol (20), the synthesis of the designated payload (**5**) was scaled up and proceeded smoothly on a 100-g scale. In order to test different cleavage mechanisms and linker hydrophilicities in combination with the payload, the following six linkers were selected for evaluation studies (for the molecular stuctures of the respective linker-drugs **LD1** to **LD6**, see Fig. 2): Val-Cit-PAB, a cathepsin-cleavable self-immolative linker leading to linker-drug **LD1**; a very short non-cleavable linker meant to keep the payload at a minimal distance from the antibody surface for enhanced steric protection leading to linker-drug **LD2** (21); a medium-length polyethylene glycol (PEG)-containing noncleavable linker furnishing linker-drug **LD3**; a glucuronidase cleavable linker (22) affording linker-drug **LD4**; Val-Ala-PAB(C–C glucuronic acid) (23), a cathepsin-cleavable self-immolative linker with enhanced solubility leading to linker-drug **LD5**; and a cathepsin-cleavable self-immolative linker with enhanced solubility and stability (22, 23) furnishing linker-drug

Significance

A number of antibody–drug conjugates (ADCs) with varying linkers carrying an uncialamycin analogue as payload were synthesized and tested for their cytotoxicity in vitro and in PDX mouse models. Importantly, a number of these enediyne-containing ADCs were found to exhibit potent and selective in vivo and in vitro cytotoxicities and also displayed a significant bystander killing effect. The latter finding is of particular importance since the currently approved enediyne ADCs (featuring an N-acetylated calicheamicin γ_1^I derivative as payload) are known not to induce bystander killing, thus lacking a possibly beneficial characteristic that could potentially improve the efficacy of oncological therapies.

Author contributions: K.C.N. and J.G. designed research; S. Rigol, E.N.P., D.D., Y.L., S. Rout, A.W.S., D.H., B.L., C.G., H.S., J.T., N.B., A.M.V., J.S., C.L., M.A., H.F., A.D., H.K., N.T., and M.P. performed research; and K.C.N., S. Rigol, and J.G. wrote the paper.

Reviewers: E.J.C., Harvard University; S.G., Juva Research; S.J.M., Yale University; and I.P., University of Cambridge.

The authors declare no competing interest.

[1]To whom correspondence may be addressed. Email: kcn@rice.edu or julia.gavrilyuk@gmail.com.

[2]Former employees of AbbVie Inc., South San Francisco, CA 94080.

This article contains supporting information online at https://www.pnas.org/lookup/suppl/doi:10.1073/pnas.2107042118/-/DCSupplemental.

Published June 21, 2021.

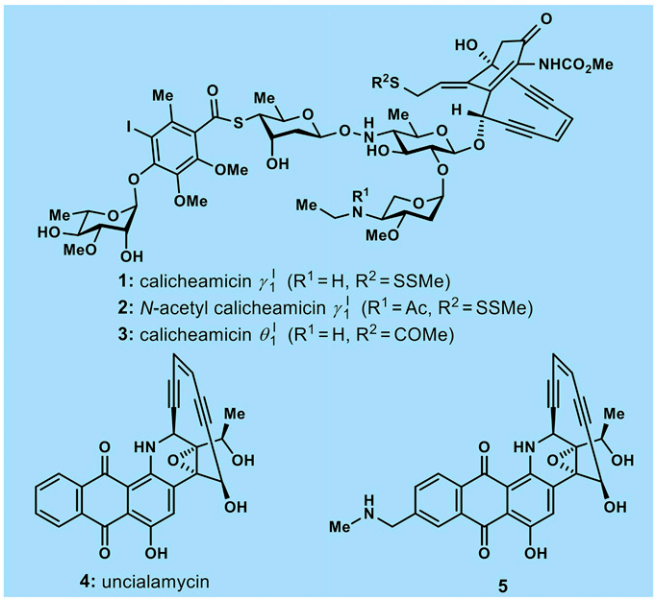

Fig. 1. Molecular structures of natural product calicheamicin γ_1^I (**1**), *N*-acetyl calicheamicin γ_1^I (**2**), totally synthetic calicheamicin θ_1^I (**3**), natural product uncialamycin (**4**), and potent uncialamycin analog.

LD6. The synthesis of the linker-drugs was performed using previously reported advanced linker intermediates (22–25).

Linker-drugs **LD1** and **LD2** were synthesized as summarized in Scheme 1 *A* and *B*, respectively. Thus, methylamino uncialamycin analog **5** was coupled with Fmoc-protected Val-Cit-PAB-4-nitrophenylcarbonate (**6**) in the presence of HOBt and Hünig's base (*i*-Pr_2EtN) to afford carbamate **7** in 75% yield. Fmoc cleavage from the latter (Et_2NH, 92% yield) led to intermediate free amine **8**, whose coupling with *N*-(α-maleimidoacetoxy)succinimide (**9**) as facilitated with *i*-Pr_2EtN and HOBt furnished linker-drug **LD1** in 31% yield. Linker-drug **LD2** was similarly prepared from methylamino uncialamycin analog **5** through coupling with activated ester **9** as induced by *i*-Pr_2EtN and HOBt (6% yield, unoptimized), as shown in Scheme 1*B*.

Linker-drug **LD3** was constructed from methylamino uncialamycin analog **5** and maleimido-PEG_8-carboxylic acid (**10**) in a single step as brought about by *i*-Pr_2EtN and HATU (33% yield), as shown in Scheme 2*A*. Scheme 2*B* summarizes the synthesis of the more sophisticated linker-drug **LD4**. Thus, coupling of the previously reported D-glucuronic acid moiety containing linker **11** (22) with uncialamycin analog **5** as facilitated by *i*-Pr_2EtN and HOBt led first to carbamate **12** and subsequently, after exposure of the latter to Et_2NH, to amine **13**. Treatment of amine **13** with LiOH led to hydrolysis of all three acetate groups and the glucuronic methyl ester moiety within **13**, furnishing polyhydroxy aminocarboxylic acid **14** in 18% overall yield for the two steps from carbamate **12**. Finally, coupling of amino acid **14** with activated ester **9** afforded linker-drug **LD4** in 18% yield, as depicted in Scheme 2*B*.

As shown in Scheme 3, the synthesis of linker-drugs **LD5** and **LD6** started with the coupling of uncialamycin analog **5** and *C*-glycoside containing activated linker **15**, as induced by *i*-Pr_2EtN and HOBt, furnishing carbamate **16** in 36% yield. Removal of the Fmoc group from **16** (Et_2NH) followed by global ester hydrolysis (LiOH) led to polyhydroxy amino acid **18** in 62% overall yield for the two steps. Coveted linker-drug **LD5** was prepared from amino acid **18** by reaction with activated ester **9** in the presence of *i*-Pr_2EtN and HATU (59% yield). Finally, linker-drug **LD6** was obtained from carboxylic acid linker-drug **LD5** through amide formation with 3,6,9,12,15,18,21,24-octaoxapentacosan-1-amine (**19**, $mPEG_8$ amine) as induced by *i*-Pr_2EtN and HATU in 59% yield, as depicted in Scheme 3.

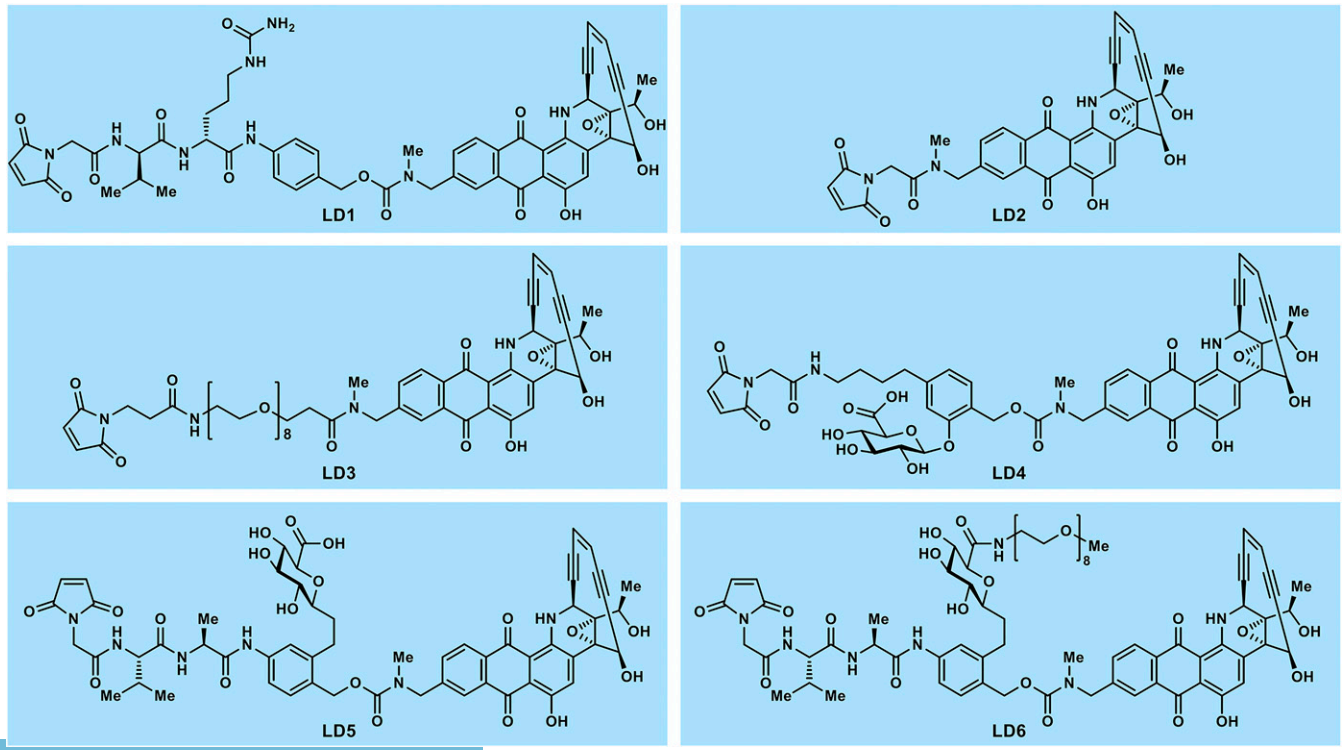

Fig. 2. Molecular structures of designed uncialamycin-based linker-drugs **LD1** to **LD6**.

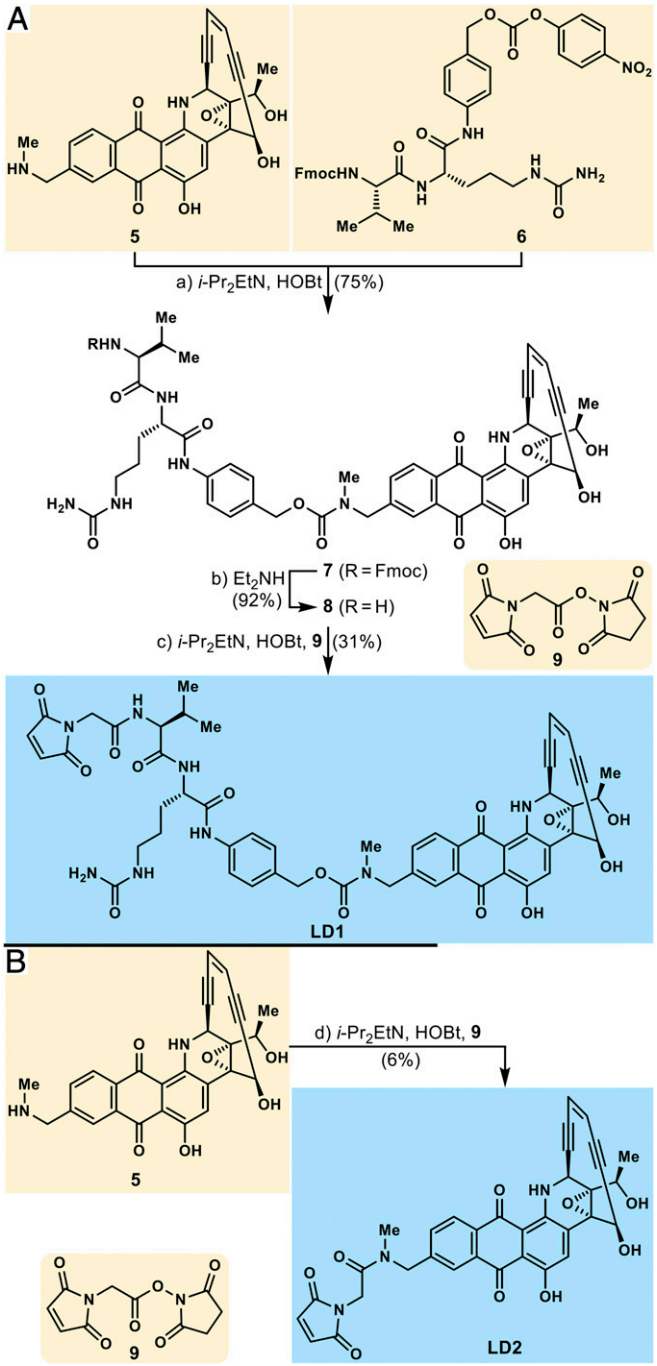

Scheme 1. Synthesis of linker-drugs **LD1** and **LD2**. Reagents and conditions: (*A*) (a) HOBt (0.5 eq), *i*-Pr_2EtN (2.0 eq), **6** (1.6 eq), DMF, 23 °C, 0.5 h, 75%; (b) Et_2NH (30 eq), MeCN, 23 °C, 1.0 h, 92%; (c) *i*-Pr_2EtN (1.4 eq), HOBt (0.5 eq), **9** (1.3 eq), DMF, 23 °C, 0.5 h; then **9** (1.3 eq), 15 min, 31%. (*B*) (d) *i*-Pr_2EtN (3.0 eq), HOBt (0.5 eq), **9** (1.3 eq), DMF, 23 °C, 0.5 h, 6%. Fmoc = fluorenylmethyloxycarbonyl; DMF = *N*,*N*-dimethylformamide; HOBt = 1*H*-1,2,3-benzotriazol-1-ol.

Antibody Conjugation of Linker-Drugs LD1 to LD6 and In Vitro Evaluation of the Resulting ADCs. The six synthesized uncialamycin linker-drugs (**LD1** to **LD6**) were conjugated to appropriate antibodies against two targets, T1 and CD46, to afford two sets of targeting ADCs (anti-T1Ab [T1Ab] and anti-CD46Ab [T2Ab]) and a nontargeting control antibody (nTAb). Model targeted antibodies were chosen to address targets either generally present in multiple types of tumors (T2 and CD46) or small-cell lung cancer tumor–specific (T1), bearing in mind our desire to evaluate the translatability of the in vitro antitumor activity to in vivo activity in patient-derived xenograft models. The nontargeting antibody recognizes artificial

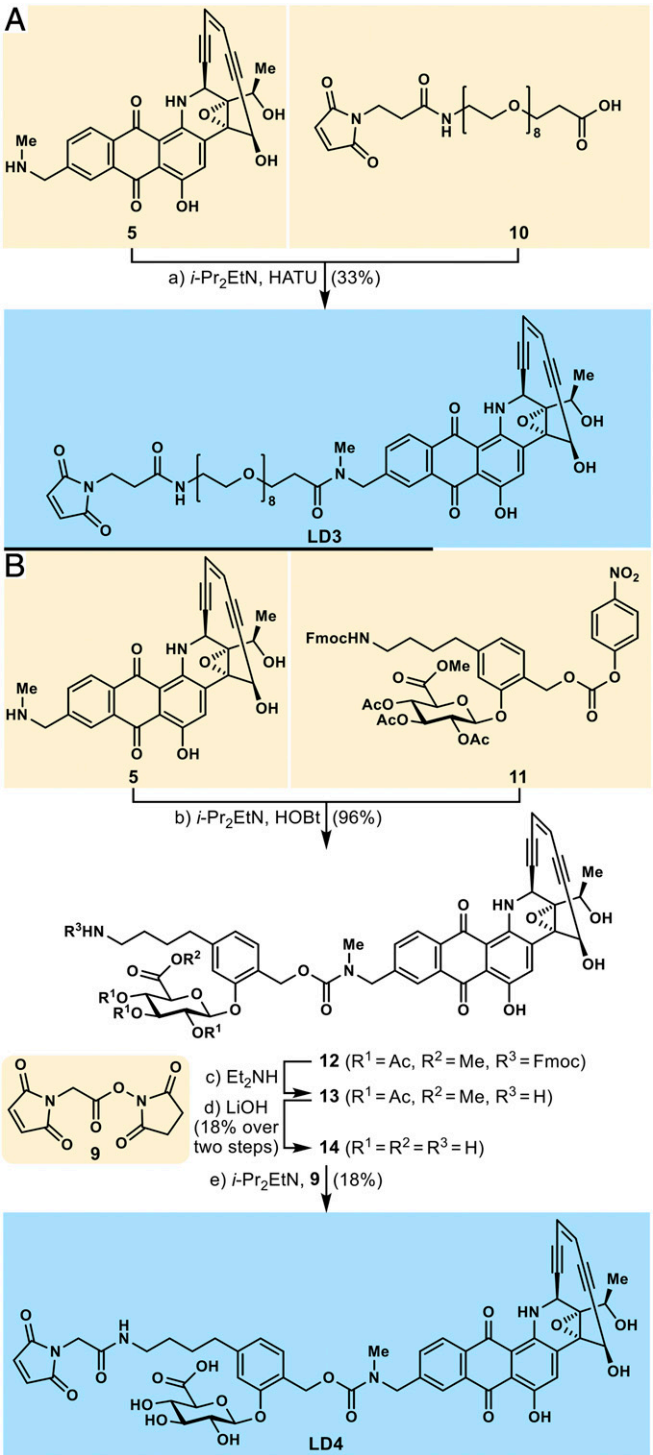

Scheme 2. Synthesis of linker-drugs **LD3** and **LD4**. Reagents and conditions: (*A*) (a) **10** (1.5 eq), *i*-Pr_2EtN (3.0 eq), HATU (1.7 eq), DMF, 0 °C, 10 min; then **5** (1.0 eq), DMF, 0 °C, 15 min, 33%. (*B*) (b) HOBt (0.5 eq), *i*-Pr_2EtN (2.0 eq), **11** (1.3 eq), DMF, 23 °C, 1.5 h, 96%; (c) Et_2NH (1.25 eq), MeCN, 23 °C, 80 min; then Et_2NH (1.25 eq), 23 °C, 50 min; (d) LiOH (15 eq), MeCN:MeOH (1:1, vol/vol), −15 °C, 0.5 h, 18% over two steps; (e) *i*-Pr_2EtN (2.0 eq), **9** (1.3 eq), DMF, 23 °C, 20 min, 18%. HATU = 1-[bis(dimethylamino)methylene]-1*H*-1,2,3-triazolo[4,5-*b*] pyridinium 3-oxide hexafluorophosphate; Ac = acetyl.

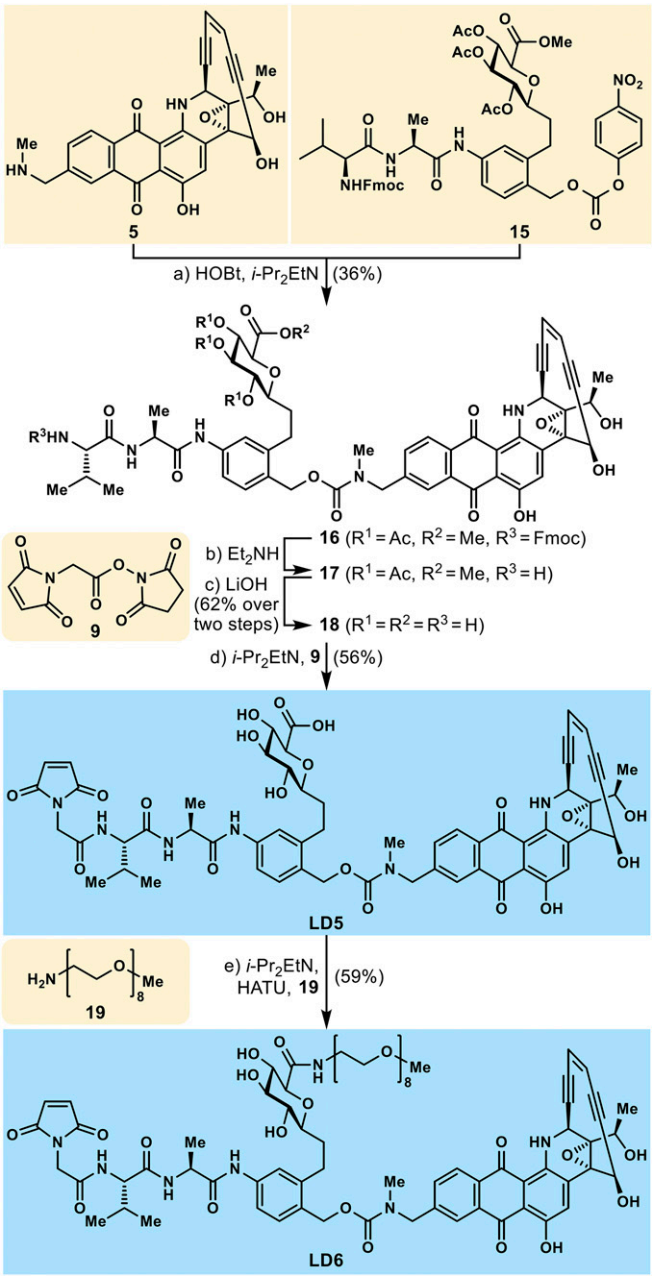

Scheme 3. Synthesis of linker-drugs **LD5** and **LD6**. Reagents and conditions: (a) HOBt (0.5 eq), *i*-Pr_2EtN (2.0 eq), **15** (1.3 eq), DMF, 23 °C, 1.5 h, 36%; (b) Et_2NH (20 eq), MeCN, 23 °C, 1 h; (c) LiOH (6.7 eq), MeCN:MeOH (1:1, vol/vol), 0 °C, 45 min, 62% over two steps; (d) *i*-Pr_2EtN (3.0 eq), **9** (1.3 eq), DMF, 23 °C, 1 h, 56%; (e) *i*-Pr_2EtN (2.0 eq), HATU (1.9 eq), **19** (1.2 eq), DMF, 0 °C, 45 min, 59%.

antigen not typically found in any human or animal tissue. Some activity observed for the nontargeting antibody illustrates the process of nonspecific antibody uptake by cells and allows for a better understanding of target-specific effects of targeted ADCs. All antibodies used in this study were engineered to have cysteine residues suitable for selective reduction and site-specific conjugation to the linker-drug. Upon completion of the conjugation, excess linker-drug was quenched with *N*-acetyl-L-cysteine (NAC) and the ADCs were subjected to mild hydrolysis conditions causing the maleimide ring to open after attachment to a cysteine residue of the antibody, thus resulting in stable linkage prohibiting possible maleimide exchange. The ADCs exhibited a uniform drug-to-antibody ratio (DAR) of 2 and had a low aggregation profile (see *SI Appendix* for details). Incidentally, due to the deep purple color of the uncialamycin payload used, all the ADC solutions were purple, indicating successful attachment of the linker-drugs onto the antibodies. All ADCs were subjected to extensive buffer exchange to eliminate any unconjugated linker-drug, which was confirmed by size-exclusion chromatography.

The uncialamycin payload, *N*-acetyl-L-cysteine-quenched linker-drugs **LD1** to **LD6**, and the corresponding set of ADCs were evaluated for in vitro plasma stability employing mouse and cynomolgus monkey plasma matrices. The linker-drugs and ADCs selected for evaluation included both cleavable as well as noncleavable linkers.

Uncialamycin analog **5** was found to be stable in mouse plasma over the course of 24 h at 37 °C. Monitoring for metabolites formation allowed the detection of only minimal amounts of molecular weight (MW)+4 Da species corresponding to a Bergman cycloaromatization (26) product and MW+20 Da species attributed to the corresponding rearranged product with added water (see *SI Appendix* for details). Only qualitative evaluation was performed at this time.

NAC-quenched linker-drugs were followed in mouse plasma (at 37 °C over 24 h) with minimal formation of metabolites observed for all evaluated linker-drugs. Qualitative assessment of observed metabolites revealed that a minimal amount of free payload was present in the samples in the case of linker-drugs containing cleavable linkers. This observation is in line with previous reports on cleavable linker release possible in mouse plasma (27). No free payload was detected in the case of linker-drug **LD2** containing a noncleavable linker. The only metabolites observed for **LD2** included minimal detectable amount of Bergman rearrangement (26) product with intact linker (MW+4 Da) and MW+22 Da species (i.e., Bergman cycloaromatization product + H_2O). Linker-drugs **LD4** and **LD5** also exhibited minimal detectable metabolites of Bergman rearrangement (26) product (MW+4 Da) and MW+22 Da (*SI Appendix*). Only qualitative assessment was done at this time to identify possible metabolites.

ADC stability evaluation in mouse plasma at 37 °C over 7 d revealed that the ADCs constructed from linker-drugs **LD4** and **LD5** featuring cleavable linkers within their molecular structures suffered over 30% decomposition after 7 d, causing significant concern for their further evaluation. The ADCs produced from **LD1** and **LD6**, also containing cleavable linker structural motifs, had acceptable levels of stability, and the ADC prepared with noncleavable linker-drug **LD2** showed only minimal levels of decomposition. Similar investigations with cynomolgus primate plasma with the same set of ADCs paralleled the observations obtained in the mouse plasma assays (*SI Appendix*).

In vitro cytotoxicity evaluation was performed using a HEK293T cell line engineered to express high levels of T1 and naturally expressing high levels of CD46. Although both targets were highly expressed in our model cell lines, we have observed differences in cytotoxic activity in vitro. That difference can be attributed to the differences in antibody internalization kinetics and intracellular processing depending on the target. We were pleased to see high levels of selectivity between targeting and nontargeting ADCs (Table 1). T1-targeting and CD46-targeting ADCs demonstrated subpicomolar to low-picomolar potencies, respectively. The observed differences in potencies were hypothesized to be attributed to different internalization and the ADC intracellular processing kinetics of the targeting antibodies. The uncialamycin ADCs were compared with the previously reported cleavable *N*-acetyl calicheamicin linker-drug (**LD7**; Fig. 3) (28) conjugated to the same T1 target and nontargeting control antibodies (i.e., T1Ab and nTAb, respectively) at DAR = 2. The uncialamycin ADCs displayed significant improvement in potency as compared to the *N*-acetyl calicheamicin control ADC (see green highlights in Tables 1 and 2).

Based on the impressive in vitro cytotoxicity and selectivity profiles coupled with the promising in vitro plasma stability, the ADCs featuring the following linker-drugs were selected for detailed in vivo evaluation in solid-tumor PDX models: linker-drugs **LD1** and **LD6**, featuring cleavable linker motifs, and linker-drugs **LD2** and **LD3**, containing noncleavable linkers. It should be noted that enediyne ADCs historically had meager success in addressing the solid-tumor problem, while being clinically efficacious in blood tumor treatment (29–34). Thus, our study was intended to set a very high bar in evaluating the potential of uncialamycin-based enediyne ADCs for the treatment of solid tumors.

Representative CD46-targeting ADCs with cleavable (**LD1**) and noncleavable (**LD2**) linker-drugs were compared to the previously disclosed cleavable *N*-acetyl calicheamicin linker-drug (**LD7**) (28) ADCs and Mylotarg as control. Thus, their cell-killing ability was evaluated in model acute myeloid leukemia cell lines OCI-AML3 and multidrug-resistant KG1. The uncialamycin ADC with cleavable linker (**T2LD1**) outperformed the *N*-acetyl calicheamicin γ_1^I ADC (Mylotarg) in the OCI-AML3 cell line and, notably, was active in multidrug-resistant KG1 cell line (Table 2). Interestingly, uncialamycin ADCs resulted in >95% reduction of viable KG1 cells, while *N*-acetyl calicheamicin γ_1^I ADC (Mylotarg) caused less than 50% reduction (*SI Appendix*).

Bystander Killing Effect Discovery. The bystander cytotoxicity effect is typically attributed to ADCs that release cell-permeable payloads and has been demonstrated for monomethyl auristatin E (MMAE) and pyrrolobenzodiazepine (PBD) ADCs in several studies (35–37). The bystander effect may have a positive impact in decreasing tumor stroma and tumor cells with no target expression that if left intact may lead to tumor regrowth. *N*-acetyl calicheamicin γ_1^I ADCs are known to not exhibit any bystander killing associated with them due to the short-lived nature of the activated biradical after release of the disulfide trigger. Thus, we were interested to evaluate and compare side-by-side our uncialamycin ADCs with *N*-acetyl calicheamicin γ_1^I ADCs, taking into consideration that the former payload presented a different activation pathway than that of the latter, albeit with the same mechanism of DNA damage stemming from biradical formation through Bergmann cycloaromatization (26). Thus, two model ADCs with cleavable linker-drugs featuring uncialamycin (**5**) and *N*-acetyl calicheamicin γ_1^I payloads were selected for the investigation: **LD1** (Scheme 1) and previously reported **LD8** (Fig. 3) (28). In the initial experiment a 1:1 mixture of T1 target-expressing and nontarget-expressing HEK293T cells were treated with titration of ADC concentrations (Fig. 4). Both T1-targeting and IgG1-nontargeting control ADCs were used. The cells were harvested and counted by flow cytometry after 48-h incubation to assess the numbers of live target-expressing and nontarget-expressing cells. As expected, nontargeting immunoglobulin G1 (IgG1) control ADCs with an uncialamycin analog or calicheamicin analog payload, respectively, did not result in marked cytotoxicity either for the target-expressing or for the nonexpressing cell line. The *N*-acetyl calicheamicin-carrying **T1LD8** ADC efficiently killed target-expressing cells while leaving the nontarget-expressing ones unaffected, supporting previously reported observations that *N*-acetyl calicheamicin γ_1^I ADCs do not exhibit a bystander killing effect (35, 38). To our surprise, **T1LD1** ADC has efficiently killed

Table 1. In vitro cytotoxicity evaluation of ADCs constructed from linker-drugs LD1 to LD6 in HEK293T cells

Antibody	Linker-drug	ADC	IC_{50}, pM
T1Ab	**LD1**	**T1LD1**	1.6
T1Ab	**LD2**	**T1LD2**	0.53
T1Ab	**LD3**	**T1LD3**	4.3
T1Ab	**LD4**	**T1LD4**	5.8
T1Ab	**LD5**	**T1LD5**	0.03
T1Ab	**LD6**	**T1LD6**	0.3
T1Ab	**LD7**	**T1LD7**	22
T2Ab (anti-CD46)	**LD1**	**T2LD1**	6.9
T2Ab (anti-CD46)	**LD2**	**T2LD2**	120
T2Ab (anti-CD46)	**LD3**	**T2LD3**	250
T2Ab (anti-CD46)	**LD4**	**T2LD4**	78
T2Ab (anti-CD46)	**LD5**	**T2LD5**	21
T2Ab (anti-CD46)	**LD6**	**T2LD6**	2.6
nTAb (nontargeting)	**LD1**	**nTLD1**	250
nTAb (nontargeting)	**LD2**	**nTLD2**	280
nTAb (nontargeting)	**LD3**	**nTLD3**	340
nTAb (nontargeting)	**LD4**	**nTLD4**	130
nTAb (nontargeting)	**LD5**	**nTLD5**	180
nTAb (nontargeting)	**LD6**	**nTLD6**	400
nTAb (nontargeting)	**LD7**	**nTLD7**	3,800

The HEK293T cell line was engineered to express high levels of target T1 and naturally expressing high levels of CD46. IC_{50}, concentration that inhibits response by 50%. Significant potency improvement compared to the *N*-acetyl calicheamicin control ADC highlighted in green.

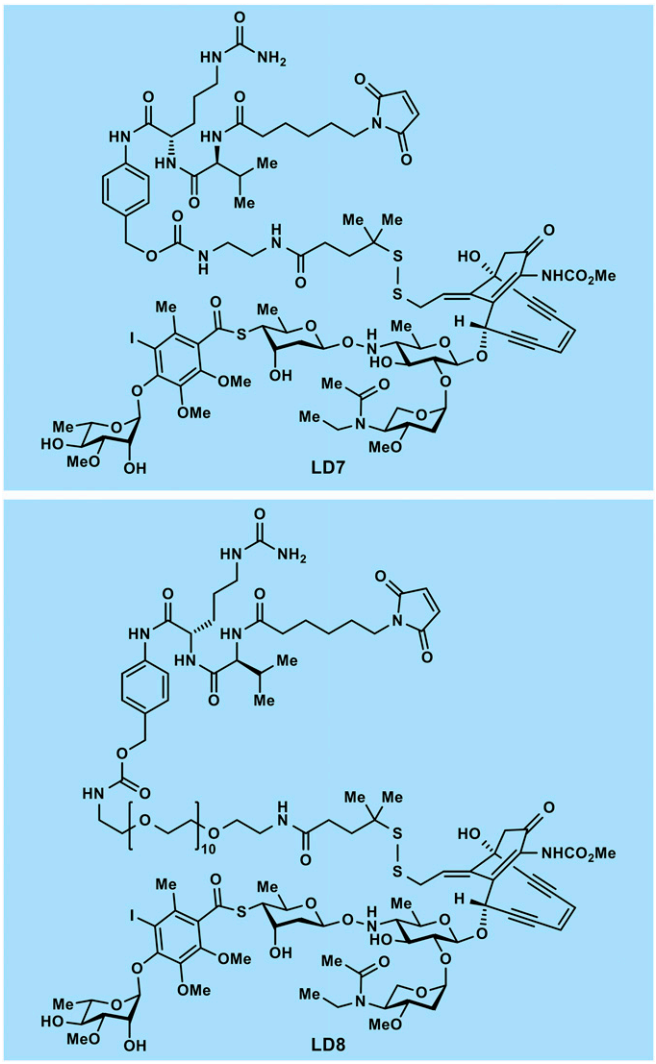

Fig. 3. Molecular structures of previously disclosed *N*-acetyl calicheamicin γ_1^I-carrying linker-drugs **LD7** and **LD8** (28).

Table 2. In vitro cytotoxicity evaluation of ADCs constructed from linker-drugs LD1 and LD2 in human acute myeloid leukemia cell lines OCI-AML3 and KG1 in comparison to *N*-acetyl calicheamicin γ_1^I ADCs

ADC	OCI-AML3 IC_{50}, nM	KG1 IC_{50}, nM
Mylotarg*	1.6	n/c
T2LD7	0.008	n/c
nTLD7	0.59	n/c
T2LD1	0.007	4.7
T2LD2	0.08	85
nTLD1	1.8	54
nTLD2	3.0	428

n/c, not converged. IC_{50}, concentration that inhibits response by 50%. Significant potency improvement compared to the *N*-acetyl calicheamicin control ADC highlighted in green.
*Gemtuzumab ozogamicin, an approved ADC consisting of an anti-CD33 monoclonal antibody and *N*-acetyl calicheamicin γ_1^I as payload.

both target-expressing and nontarget-expressing cells, indicating a strong bystander killing effect (*SI Appendix*). To further investigate this observation, the experiment was extended by modifying the ratio between target-expressing to nonexpressing cells. The ratio was changed from 1:1 to 1:2, 1:5, and 1:10, respectively, while the concentration of the ADC was kept constant at 50 pM. Similar to the initial experiment, the nontargeting IgG1 control ADCs did not have a significant impact on the cell viability of target-expressing or nonexpressing cells. While *N*-acetyl calicheamicin γ_1^I analog-based ADC **T1LD8** once again eliminated target-expressing cells, leaving nontarget-expressing cells unaffected, its uncialamycin counterpart **T1LD1** eliminated target-expressing and the majority of nontarget-expressing cells at ratios up to 1:5 (target-expressing:nontarget-expressing cells), providing further support for a pronounced bystander killing effect exhibited by the uncialamycin ADC (Fig. 4).

In Vivo Evaluation of Uncialamycin ADCs. Uncialamycin ADCs featuring cleavable (**LD1** and **LD6**) and noncleavable (**LD2** and **LD3**) linker-drugs were evaluated in vivo in two patient-derived small-cell lung cancer xenograft models that had high levels of expression of both targets T1 and T2 (CD46). ADCs with noncleavable linker-drugs **LD2** and **LD3** were found to be inactive at all evaluated dose levels. This result was in striking contrast to the established in vitro cytotoxic activity of the target-specific ADCs and prompted us to further investigate the in vivo pharmacokinetic profile of the uncialamycin ADCs. In these studies, ADCs with cleavable linker-drugs **LD1** and **LD6** demonstrated significant antitumor activity in a target-specific and dose-dependent manner. In

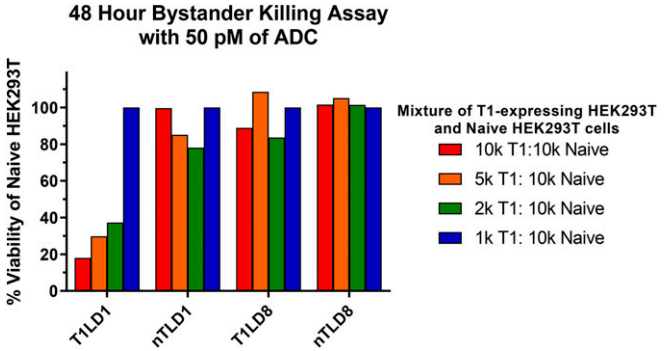

Fig. 4. Bystander killing assay of two uncialamycin ADCs (**T1LD1** and **nTLD1**) in comparison to their *N*-acetyl calicheamicin γ_1^I counterparts (**T1LD8** and **nTLD8**).

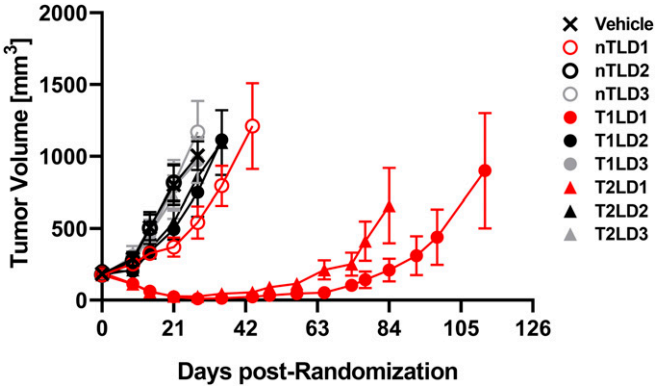

Fig. 5. Tumor volume trajectories in a LU95 small-cell lung cancer PDX model after treatment with nontargeting and targeting ADC constructs carrying linker-drugs **LD1**, **LD2**, and **LD3**, respectively, at 1.5 mg/kg doses.

LU95 (Figs. 5 and 6) and LU149 (*SI Appendix*) small-cell lung cancer PDX models **T1LD1** and **T2LD1** at 1.5 mg/kg dose had similar antitumor effects, demonstrating complete tumor regression sustained for >40 d. **T1LD1** had even greater sustained tumor regression (>80 d) at 3 mg/kg dose level in the LU149 PDX model. At 1 mg/kg dose level, **T1LD6** had similar (LU149) or slightly greater (LU95) efficacy compared with **T1LD1**. Notably, all nontargeting IgG1 ADCs exerted no antitumor activity.

In order to better understand the observed antitumor activity of the uncialamycin ADCs with cleavable vs. noncleavable linker-drugs, a pharmacokinetics study in NOD/SCID mice was performed. Each group of female NOD/SCID mice was given a single intravenous bolus dose of 5 mg/kg of either **nTLD1**, **T1LD1**, **T1LD2** or **T1LD6**. Blood samples were collected and bioanalysis of total antibody and conjugated drug concentrations was performed (see *SI Appendix* for full experimental details). All ADCs with cleavable linker-drugs were found to have ADC half-lives ranging from 0.7 to 2 d, with the **T1LD6** ADC having the shortest half-life, while the ADC with noncleavable linker-drug **LD2** had a half-life of 11.8 d (*SI Appendix*). Rapid increase in total antibody to ADC ratio was characteristic of all ADCs in this study and closely resembled pharmacokinetic profiles reported for *N*-acetyl calicheamicin γ_1^I ADCs in mice (39, 40).

Conclusion

A diverse set of uncialamycin ADCs featuring a variety of linker cleavage mechanisms have been constructed and evaluated. It was discovered that an uncialamycin ADC (**T1LD1**) containing a

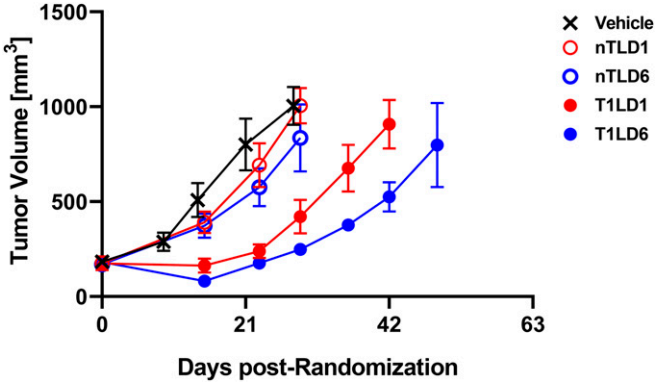

Fig. 6. Tumor volume trajectories in a LU95 small-cell lung cancer PDX model after treatment with nontargeting and targeting ADC constructs carrying linker-drugs **LD1** and **LD6**, respectively, at 1.0 mg/kg doses.

cleavable linker-drug exhibits significant bystander killing effect at the target-expressing:nontarget-expressing cell ratio of 1:5 at 50 pM ADC concentration. This observation is in contrast to the absence of such a bystander killing effect in *N*-acetyl calicheamicin γ_1^I–containing ADCs and presents an intriguing opportunity in the tumor-targeting therapeutics development area. Both payloads, *N*-acetyl calicheamicin γ_1^I and uncialamycin, belong to the DNA damaging class of enediynes, yet the subtle differences in their antitumor effects may be exploited to fine-tune their therapeutic value toward specific cancer indications. In particular, uncialamycin ADCs demonstrated marked antitumor activity in solid-tumor PDX models. Significantly, uncialamycin-containing ADCs with cleavable linker-drugs were found to produce durable target-specific tumor regression effects in small-cell lung cancer PDX mouse models. These preliminary results warrant future investigations of uncialamycin analogs as payloads for the development of powerful targeted anticancer therapeutics.

Data Availability. All study data are included in the article and/or *SI Appendix*.

ACKNOWLEDGMENTS. This work was supported by the Cancer Prevention & Research Institute of Texas (CPRIT), The Welch Foundation (grant C-1819), and AbbVie. K.C.N. is a CPRIT Scholar in cancer research.

1. P. Ehrlich, Die Aufgaben der Chemotherapie. *Frankfurter Zeitung und Handelsblatt*, 4 September 1906, **51**, No. 244, Zweites Morgenblatt, Feuilleton.
2. L. M. Hinman *et al.*, Preparation and characterization of monoclonal antibody conjugates of the calicheamicins: A novel and potent family of antitumor antibiotics. *Cancer Res.* **53**, 3336–3342 (1993).
3. P. R. Hamann *et al.*, Gemtuzumab ozogamicin, a potent and selective anti-CD33 antibody-calicheamicin conjugate for treatment of acute myeloid leukemia. *Bioconjug. Chem.* **13**, 47–58 (2002).
4. D. J. Newman, Natural product based antibody drug conjugates: Clinical status as of November 9, 2020. *J. Nat. Prod.* **84**, 917–931 (2021).
5. J. A. Francisco *et al.*, cAC10-vcMMAE, an anti-CD30-monomethyl auristatin E conjugate with potent and selective antitumor activity. *Blood* **102**, 1458–1465 (2003).
6. J. M. Lambert, R. V. J. Chari, Ado-trastuzumab Emtansine (T-DM1): An antibody-drug conjugate (ADC) for HER2-positive breast cancer. *J. Med. Chem.* **57**, 6949–6964 (2014).
7. J. F. DiJoseph *et al.*, Antibody-targeted chemotherapy with CMC-544: A CD22-targeted immunoconjugate of calicheamicin for the treatment of B-lymphoid malignancies. *Blood* **103**, 1807–1814 (2004).
8. D. Dornan *et al.*, Therapeutic potential of an anti-CD79b antibody-drug conjugate, anti-CD79b-vc-MMAE, for the treatment of non-Hodgkin lymphoma. *Blood* **114**, 2721–2729 (2009).
9. P. M. Challita-Eid *et al.*, Enfortumab vedotin antibody–drug conjugate targeting nectin-4 is a highly potent therapeutic agent in multiple preclinical cancer models. *Cancer Res.* **76**, 3003–3013 (2016).
10. Y. Ogitani *et al.*, DS-8201a, a novel HER2-targeting ADC with a novel DNA topoisomerase I inhibitor, demonstrates a promising antitumor efficacy with differentiation from T-DM1. *Clin. Cancer Res.* **22**, 5097–5108 (2016).
11. T. M. Cardillo, S. V. Govindan, R. M. Sharkey, P. Trisal, D. M. Goldenberg, Humanized anti-trop-2 IgG-SN-38 conjugate for effective treatment of diverse epithelial cancers: Preclinical studies in human cancer xenograft models and monkeys. *Clin. Cancer Res.* **17**, 3157–3169 (2011).
12. Y.-T. Tai *et al.*, Novel anti-B-cell maturation antigen antibody-drug conjugate (GSK2857916) selectively induces killing of multiple myeloma. *Blood* **123**, 3128–3138 (2014).
13. R. F. Alderson *et al.*, CAT-8015: A second-generation *pseudomonas* exotoxin A-based immunotherapy targeting CD22-expressing hematologic malignancies. *Clin. Cancer Res.* **15**, 832–839 (2009).
14. F. Zammarchi *et al.*, ADCT-402, a PBD dimer-containing antibody drug conjugate targeting CD19-expressing malignancies. *Blood* **131**, 1094–1105 (2018).
15. H. N. Lode *et al.*, Targeted therapy with a novel enediyene antibiotic calicheamicin θ_1^I effectively suppresses growth and dissemination of liver metastases in a syngeneic model of murine neuroblastoma. *Cancer Res.* **58**, 2925–2928 (1998).
16. K. C. Nicolaou *et al.*, Calicheamicin θ_1^I: A rationally designed molecule with extremely potent and selective DNA cleaving properties and apoptosis inducing activity. *Angew. Chem. Int. Ed. Engl.* **33**, 183–186 (1994).
17. K. C. Nicolaou, H. Zhang, J. S. Chen, J. J. Crawford, L. Pasunoori, Total synthesis and stereochemistry of uncialamycin. *Angew. Chem. Int. Ed.* **46**, 4704–4707 (2007).
18. K. C. Nicolaou, J. S. Chen, H. Zhang, A. Montero, Asymmetric synthesis and biological properties of uncialamycin and 26-*epi*-uncialamycin. *Angew. Chem. Int. Ed.* **47**, 185–189 (2008).
19. J. Davies *et al.*, Uncialamycin, a new enediyne antibiotic. *Org. Lett.* **7**, 5233–5236 (2005).
20. K. C. Nicolaou *et al.*, Streamlined total synthesis of uncialamycin and its application to the synthesis of designed analogues for biological investigations. *J. Am. Chem. Soc.* **138**, 8235–8246 (2016).
21. D. Su *et al.*, Modulating antibody–drug conjugate payload metabolism by conjugation site and linker modification. *Bioconjug. Chem.* **29**, 1155–1167 (2018).
22. P. J. Burke *et al.*, Optimization of a PEGylated glucuronide-monomethylauristatin E linker for antibody–drug conjugates. *Mol. Cancer Ther.* **16**, 116–123 (2017).
23. E. R. Boghaert, A. J. Souers, A. C. Phillips, A. S. Judd, M. Bruncko, "Anti-EGFR antibody drug conjugates." Patent WO 2017214282 A1 (2017).
24. Y. Mao, P. Moquist, A. Choudhury, W. Doubleday, "Process for the preparation of glucuronide drug-linkers and intermediates thereof." Patent WO 2018175994 A1 (2018).
25. J. D. Bargh, A. Isidro-Llobet, J. S. Parker, D. R. Spring, Cleavable linkers in antibody-drug conjugates. *Chem. Soc. Rev.* **48**, 4361–4374 (2019).
26. R. R. Jones, R. G. Bergman, *p*-Benzyne. Generation as an intermediate in a thermal isomerization reaction and trapping evidence for the 1,4-benzenediyl structure. *J. Am. Chem. Soc.* **94**, 660–661 (1972).
27. M. Dorywalska *et al.*, Effect of attachment site on stability of cleavable antibody drug conjugates. *Bioconjug. Chem.* **26**, 650–659 (2015).
28. J. Gavrilyuk, V. N. Sisodiya, "Calicheamicin constructs and methods of use." Patent WO 2016172273 A1 (2016).
29. Y. N. Lamb, Inotuzumab ozogamicin: First global approval. *Drugs* **77**, 1603–1610 (2017).
30. J. Baron, E. S. Wang, Gemtuzumab ozogamicin for the treatment of acute myeloid leukemia. *Expert Rev. Clin. Pharmacol.* **11**, 549–559 (2018).
31. J. Hitzler, E. Estey, Gemtuzumab ozogamicin in acute myeloid leukemia: Act 2, with perhaps more to come. *Haematologica* **104**, 7–9 (2019).
32. R. G. Dushin, "Calicheamicins as antibody–drug conjugate (ADC) payloads" in *Cytotoxic Payloads for Antibody–Drug Conjugates*, D. E. Thurston, P. J. M. Jackson, Eds. (The Royal Society of Chemistry, 2019), pp. 259–278.
33. J. Wynne, D. Wright, W. Stock, Inotuzumab: From preclinical development to success in B-cell acute lymphoblastic leukemia. *Blood Adv.* **3**, 96–104 (2019).
34. A. Adhikari, B. Shen, C. Rader, Challenges and opportunities to develop enediyne natural products as payloads for antibody-drug conjugates. *Antibody Ther.* **4**, 1–15 (2021).
35. A. H. Staudacher, M. P. Brown, Antibody drug conjugates and bystander killing: Is antigen-dependent internalisation required? *Br. J. Cancer* **117**, 1736–1742 (2017).
36. A. P. Singh, S. Sharma, D. K. Shah, Quantitative characterization of in vitro bystander effect of antibody-drug conjugates. *J. Pharmacokinet. Pharmacodyn.* **43**, 567–582 (2016).
37. J. H. Byun, I. H. Jung, Modeling to capture bystander-killing effect by released payload in target positive tumor cells. *BMC Cancer* **19**, 194 (2019).
38. J. F. Dijoseph *et al.*, CD20-specific antibody-targeted chemotherapy of non-Hodgkin's B-cell lymphoma using calicheamicin-conjugated rituximab. *Cancer Immunol. Immunother.* **56**, 1107–1117 (2007).
39. M. Buckwalter, J. A. Dowell, J. Korth-Bradley, B. Gorovits, P. R. Mayer, Pharmacokinetics of gemtuzumab ozogamicin as a single-agent treatment of pediatric patients with refractory or relapsed acute myeloid leukemia. *J. Clin. Pharmacol.* **44**, 873–880 (2004).
40. Committee for Medicinal Products for Human Use (European Medicines Agency), Assessment report Mylotarg (2018). https://www.ema.europa.eu/en/documents/assessment-report/mylotarg-epar-public-assessment-report_en.pdf. Accessed 4 March 2021.